Endocrinology. First published September 1, 2005 as doi:10.1210/en.2005-0578

# Selective tissue uptake of AgRP (82-131) and its modulation by fasting

Weihong Pan, Abba J. Kastin, Yongmei Yu, Courtney M. Cain, Tammy Fairburn, Adrian M. Stütz, Christopher Morrison, George Argyropoulos

Pennington Biomedical Research Center, LSU System, Baton Rouge, LA, USA



Corresponding author:
Weihong Pan, M.D., Ph.D.
PBRC
6400 Perkins Road
Baton Rouge, LA 70808
Tel. (225) 763-2707
Fax (225) 763-0261
e-mail: weihong.pan@pbrc.edu

**ABSTRACT**

The blood concentration of agouti-related protein (AgRP), a protein related to hyperphagia and obesity, is increased in obese human and fasted lean subjects. Since there is no saturable transport system at the blood-brain barrier (BBB) for circulating AgRP to reach its CNS target, uptake of AgRP by peripheral organs might be physiologically meaningful. Using the biologically active fragment AgRP (82-131), we determined the pharmacokinetics of its radioactively labeled tracer after intravenous bolus injection, and compared it with that of the vascular marker albumin. AgRP enters peripheral organs at different influx rates, all of which were higher than into brain and spinal cord. At 10 min after intravenous injection, the radioactivity recovered in the liver, which had the fastest influx rate for AgRP, represented intact $^{125}$I-AgRP. The adrenal gland had a moderately fast uptake (but the highest initial volume of distribution), followed by the heart, lungs, and skeletal muscle. By comparison, epididymal fat, testis, and pancreas had low permeability to AgRP. Saturation of influx was determined by co-administration of excess unlabeled AgRP and was shown to be present in the liver and adrenal gland. The influx rate and initial volume of distribution did not show a linear correlation with vascular permeability or regional blood flow. AgRP uptake by the liver and epididymal fat was significantly increased by overnight fasting whereas that by the adrenal gland was significantly decreased in fasted mice. Thus, the differential uptake of AgRP by peripheral organs could be a regulated process that is modulated by food deprivation.

*Keywords*: AgRP; blood-brain barrier; tissue distribution; influx rate; obesity; fasting

## INTRODUCTION

Obese humans (1) as well as fasted rats (2) and humans (3) all have increased plasma levels of the agouti-related protein (AgRP). Obesity and its complications cause serious health problems, but strategies to counteract excessive weight gain are limited (4). AgRP is a powerful enhancer of food intake (5;6) and its encoding gene is implicated in obesity. We have shown that single nucleotide polymorphisms (SNPs) of AgRP result in decreased promoter activity or protein functionality, and that these SNPs are associated with reduced obesity, a lower incidence of type 2 diabetes, and the prevention of late-onset obesity in humans (7-9). AgRP is expressed in the arcuate nucleus and adrenal gland (10;11) and is upregulated in *ob/ob* and *db/db* mice (12;13). Transgenic mice overexpressing AgRP are hyperphagic and obese, and exhibit hyperinsulinemia, late-onset hyperglycemia, pancreatic islet hyperplasia, and reduced corticosterone levels (14).

Most of the actions of AgRP take place in the hypothalamus, where it is an endogenous antagonist to MCR-3 and MCR-4 receptors. In addition to the full-length protein, C-terminal fragments are also bioactive. Intracerebroventricular injection of AgRP(82-131) induces hyperphagia and obesity in animals (15 - 17). The same fragment increases food intake and reduces spontaneous locomotor activity (18), and reduces energy expenditure (19). The effect of AgRP(87-132) in reduction of food intake is mediated by its binding to melanocortin receptors MC3R, MC4R, and MC5R, counteracting α-MSH (20). With this evidence for the biological activity of amino acid residues in the 82-131 region of AgRP, we used AgRP(82-131) in our study. However, it aggregates and crosses the blood-brain barrier (BBB) only at a slow rate (21). This could explain why

intracerebroventricular AgRP is more potent than short exposure to peripheral AgRP for stimulation of food intake and reduction of energy expenditure (22).

Nonetheless, emerging evidence indicates not only that hypothalamic AgRP contributes to obesity, but that peripheral AgRP also plays a significant role in energy balance. Apart from the arcuate nucleus of the hypothalamus and subthalamic nucleus, a shorter transcript of AgRP mRNA, missing the 5' non coding exon but still resulting in full-length protein, is expressed in the adrenal gland, testis, kidney, and the lungs (23). AgRP can block the action of α-MSH in the adrenal gland and fat tissue (24;25) and inhibit ACTH-induced cortisol production in cultured bovine adrenal cells (26). After electroporation of AgRP cDNA into the leg muscle, there are increases in food intake, body weight, and serum AgRP levels (27). The effects are likely mediated by peripheral receptors, as MCR3 and MCR4 are present in the rat adrenal gland (28) and MC4R expression also occurs in adult rat heart, lung, kidney, and testis (29).

On the one hand, AgRP is produced by selective organs and possibly exerts autocrine or paracrine roles. The mRNA of AgRP in fasted mice is higher in the hypothalamus, adrenal gland, and testis, but lower in epididymal fat (30). The changes in AgRP expression after food deprivation could in turn affect energy balance. On the other hand, AgRP could also be an endocrine signal since the endogenous protein is detectable in circulating blood. AgRP plasma levels are higher in obese individuals (1) and are affected by fasting in humans and rats (2). In our recent fasting studies in mice, there was also an elevation in blood concentrations of AgRP protein that correlated with increased AgRP

mRNA in selective organs (30). We therefore determined whether the kinetics of peripheral organ uptake of AgRP is related to its actions in fed and fasted states.

Mouse $^{125}$I-AgRP(82-131) was used in this study because it is the commonly used form for pharmacological assays and is biologically active. The relative stability of AgRP during the study period enabled the measurement of the influx rate and volume of distribution in the brain and peripheral organs. We found an important, although small, uptake of AgRP by the brain, supporting our previous observation that AgRP can slowly penetrate the BBB to affect CNS function. Moreover, there was high uptake of AgRP by liver, adrenal gland, heart, lungs, and skeletal muscle. Part of the differential distribution of blood-borne AgRP in peripheral organs was a saturable process, as seen in the liver and adrenal gland. Of particular interest, overnight fasting caused a statistically significant increase in the uptake of AgRP by liver and epididymal fat, and decrease in the adrenal gland. Therefore, organ-specific uptake suggests that circulating AgRP is physiologically important.

## MATERIALS AND METHODS

Carrier-free mouse AgRP (82-131)-$NH_2$ was purchased from Phoenix Pharmaceuticals (Belmont, CA). The peptide was radioactively labeled with $^{125}$I by the chloramine-T method. In detail, 10 - 40 μg of AgRP (82-131) was incubated with 1 mCi of $^{125}$I (Perkin Elmer, Boston, MA) after adjusting pH to 7.4 by 0.5 M phosphate buffer. The reaction was carried out in the presence of chloramine-T (final concentration of 0.13 mg/ml) for 1 min, and terminated by addition of sodium metabisulfite (final concentration of 0.5

mg/ml). The iodination mixture was purified by elution on a column of Sephadex G-10 to remove free $^{125}$I. Similarly, bovine serum albumin was radioactively labeled with $^{131}$I by the chloramine-T method and purified on a Sephadex G-10 column. The specific activities of $^{125}$I-AgRP and $^{131}$I-albumin were about 46 Ci/g and 6 Ci/g, respectively. They were aliquoted and stored at –20 $^{o}$C until use. At the time of study, the acid precipitability of both compounds was greater than 98%.

Most studies used 8-12 week-old male C57BL/6J (C57) mice (mean weight of 24.7 g) unless specified. The C57 mice were bred in our animal care facility. The CD1 mice were purchased from Charles River at 4-6 weeks of age and used at least one week after acclimation. The mice were anesthetized by intraperitoneal injection of a mixture of ketamine /xylazine /acepromazine. The protocol was approved by the Institutional Animal Care and Use Committee.

To determine how fast and how much $^{125}$I-AgRP was taken up from blood, multiple-time regression analysis (31;32) was performed. Two groups of mice were studied: those receiving radioactively labeled tracer only and those receiving excess unlabeled AgRP (1 μg/mouse) to test the possible presence of a saturable transport system (n = 8 - 10 /group). In each group, $^{125}$I-AgRP and $^{131}$I-albumin were injected into the exposed left jugular vein at time 0 in a bolus of 100 μl of lactated Ringer's solution containing 1% albumin (LR/BSA). About 20,000 cpm /μl of radiotracers were injected, corresponding to about 19 ng of $^{125}$I-AgRP and 225 ng of $^{131}$I-albumin in each mouse, respectively. At various time points between 1 and 30 min (resulting in the longest calculated exposure

time of more than 50 min, as explained in the description of data analysis below), blood was obtained by transection of the carotid artery, and the mouse was decapitated 20 – 30 sec later. One mouse was used for each time point within the group. The experiment was repeated four times, using a different group of mice each time. The following organs or tissues were harvested and weighed: brain, spinal cord, heart, lungs, liver, spleen, pancreas, adrenal gland, kidney, epididymal fat, soleus muscle, and testis. For the brain, nine different regions were dissected: frontal cortex, parietal cortex, occipital cortex, striatum, thalamus, hypothalamus, midbrain, pons/medulla, and cerebellum. The spinal cord was divided into cervical, thoracic, and lumbar regions. The radioactivity in the tissue and 50 μl of serum was measured in a γ-counter. The tissue/serum ratio of radioactivity was calculated for each mouse, which represented each time point. The linear regression correlation between tissue/serum ratio and exposure time was determined for each group. The exposure time is the integral of serum radioactivity from time 0 to time t divided by the theoretical radioactivity at time t, and represents a steady-state value if the blood concentration of $^{125}$I-AgRP remained constant (32).

Based on established methods, the linear regression correlation between tissue uptake from blood and the exposure time was determined by the least squares method with the Prism 3.0 program (GraphPad, Inc., San Diego, CA). The unidirectional influx rate Ki is reflected by the slope of this linear regression line. This indicates the influx rate and is expressed as a mean with its standard error. The initial volume of distribution Vi reflects the binding affinity as well as vascular space in each organ. It is first determined whether there are differences between or among slopes, and if not, whether there are differences

between or among intercepts. More than two slopes are compared by analysis of variance followed by Newman-Keuls range test with the standard deviation taken as the standard error term. Because two means (the slope and the intercept) were calculated from the data, n-1 was used as the value for sample size (33).

To determine the stability of $^{125}$I-AgRP *in-vivo*, mice received an intravenous injection of $^{125}$I-AgRP in LR/BSA at time 0, and were decapitated 10 min after arterial blood was collected. Reversed-phase high performance liquid chromatography (HPLC) was performed on serum and the supernatant of tissue homogenates after they were passed through 0.4 μm syringe filters. The mobile phase was acetonitrile with 0.1% trifluoroacetic acid, and a linear gradient of 10% to 100% over 30 min was used. The elution position of intact $^{125}$I-AgRP correlated with the fractions of the stock solution and was confirmed by greater than 95% acid precipitability with 15% trichloroacetic acid. To correct for ex-vivo degradation during sample collection and tissue homogenization, a processing control was prepared in parallel by addition of $^{125}$I-AgRP to the test tubes.

To assess the actual amount of $^{125}$I-AgRP taken up by parenchyma as compared with that trapped in the vasculature, the capillary depletion procedure was performed on samples collected 10 min after intravenous injection of $^{125}$I-AgRP and $^{131}$I-albumin. One group of mice (n = 4) was decapitated immediately after blood was collected from the abdominal aorta whereas another group of mice (n = 5) received 25 ml of lactated Ringer's solution by intracardial perfusion during the time between blood collection and decapitation. The cerebral cortex from each individual mouse was dissected, weighed, and homogenized in

0.7 ml of capillary buffer (34). The homogenate was mixed thoroughly with 1.7 ml of 26% dextran and centrifuged at 6500 g for 30 min in a swing bucket rotor. The resultant pellet (capillaries) and supernatant (brain parenchyma) were carefully separated, and their radioactivity was measured by a dual-channel program in the γ-counter. The tissue/serum ratio of radioactivity for $^{125}$I-AgRP and $^{131}$I-albumin was calculated independently. One-way analysis of variance was performed between the groups.

In the fasting studies, the control mice were fed a low fat chow diet (12.1 kcal %fat, mouse Labdiet #5001, Purina Mills, St. Louis, MO) after weaning. The mice were kept on a 12/12 h light cycle (lights on 6 am and off 6 pm). Overnight fasting (17 h) was achieved by food removal at 5 pm on the day before transport measurement, and injection of the radioactive tracer injection was started at 11 am immediately after anesthesia. In the single-time uptake study with C57 mice, each mouse received $^{125}$I-AgRP in 100 μl of LR/BSA at time 0 and was decapitated 10 min after arterial blood was collected. Brain, heart, lungs, liver, pancreas, adrenal gland, epididymal fat, soleus muscle, and testis were collected and weighed. The mean and standard error of tissue/serum radioactivity were obtained, and one-way analysis of variance was performed. In the multiple-time regression analysis on CD1 mice, $^{125}$I-AgRP was given at time 0, groups of mice were decapitated at various time points between 1 and 20 min, as specified above, and final analysis was performed by the least squares method with the GraphPad program.

## RESULTS

### 1. Tissue uptake of $^{125}$I-AgRP showed large differences among organs

The decay of radioactivity in serum fit a one-phase exponential decay model; the influx rates were 0.117 ± 0.047 for the group with $^{125}$I-AgRP only and 0.093 ± 0.025 for the group with additional unlabeled AgRP at 1 μg/mouse. The half-lives of $^{125}$I-AgRP were 5.9 min and 7.4 min, respectively. Since the regression correlation between the tissue uptake from blood and the calculated exposure time was linear within 30 min actual time of iv injection, we chose this period to conduct most of the kinetics studies, with the resulting calculated exposure time extending over 50 min. Table 1 lists the pharmacokinetic parameters (Ki and Vi) in different regions for both AgRP and the vascular control albumin.

Table 1. Tissue-specific uptake of $^{125}$I-AgRP as compared with the paracellular permeability marker $^{131}$I-albumin.

| *Region* | *AgRP Ki (μl/g-min)* | *AgRP Vi (μl/g)* | *Albumin Ki (μl/g-min)* | *Albumin Vi (μl/g)* |
|---|---|---|---|---|
| Brain | 0.141 ± 0.025 | 12.55 ± 1.00 | 0.023 ± 0.029 | 8.16 ± 0.48 |
| Frontal lobe | 0.047 ± 0.040 | 11.88 ± 0.95 | 0.025 ± 0.034 | 8.22 ± 0.55 |
| Parietal lobe | 0.194 ± 0.052 | 8.34 ± 1.34 | 0.061 ± 0.044 | 5.91 ± 0.71 |
| Occipital lobe | 0.497 ± 0.105 | 7.65 ± 2.56 | 0.077 ± 0.149 | 9.43 ± 2.43 |
| Striatum | 0.306 ± 0.070 | 11.71 ± 1.42 | -0.057 ± 0.028 | 7.05 ± 0.46 |
| Thalamus | 0.218 ± 0.153 | 14.73 ± 3.15 | 0.011 ± 0.027 | 6.35 ± 0.43 |
| Hypothalamus | 0.118 ± 0.038 | 13.46 ± 0.89 | 0.004 ± 0.053 | 7.36 ± 0.86 |
| Midbrain | 0.037 ± 0.076 | 13.86 ± 1.69 | 0.114 ± 0.089 | 8.34 ± 1.45 |
| Pons/medulla | -0.003 ± 0.078 | 18.42 ± 1.86 | 0.007 ± 0.060 | 10.83 ± 0.986 |
| Cerebellum | 0.078 ± 0.076 | 16.04 ± 1.82 | -0.046 ± 0.055 | 10.94 ± 0.89 |
| Spinal cord | 0.258 ± 0.042 | 11.20 ± 1.00 | 0.057 ± 0.038 | 6.59 ± 0.62 |
| Cervical | 0.40 ± 0.09 | 14.12 ± 2.34 | 0.093 ± 0.070 | 8.62 ± 1.14 |
| Thoracic | 0.18 ± 0.06 | 7.01 ± 1.49 | 0.022 ± 0.054 | 5.13 ± 0.88 |
| Lumbar | 0.15 ± 0.11 | 12.73 ± 2.68 | 0.035 ± 0.073 | 7.31 ± 1.18 |
| Liver | 59.79 ± 4.27 | 539.3 ± 97.19 | 1.093 ± 0.208 | 58.99 ± 3.40 |
| Adrenal gland | 12.69 ± 1.48 | 655.0 ± 35.50 | 0.513 ± 1.439 | 173.3 ± 23.46 |
| Heart | 7.24 ± 3.04 | 164.4 ± 72.78 | 1.019 ± 1.446 | 104.4 ± 23.57 |
| Lungs | 5.71 ± 2.22 | 205.3 ± 53.24 | 0.358 ± 0.529 | 73.59 ± 8.63 |
| Muscle | 3.56 ± 0.84 | 69.55 ± 20.21 | 0.376 ± 0.294 | 14.92 ± 4.79 |
| Epididymal fat | 1.00 ± 0.29 | 19.41 ± 7.02 | 0.086 ± 0.039 | 2.84 ± 0.63 |
| Testis | 0.93 ± 0.15 | 11.82 ± 3.50 | 0.303 ± 0.058 | 4.50 ± 0.94 |
| Pancreas | 0.71 ± 0.81 | 126.0 ± 19.3 | 0.044 ± 0.112 | 10.18 ± 1.83 |

Figure 1 shows that liver had the fastest entry of $^{125}$I-AgRP, with an influx rate Ki of 59.79 ± 4.27 μl/g-min and an initial volume of distribution of 539.3 ± 97.2 μl/g. GraphPad Prism 3.0 program was used to determine the difference between the Ki of the two groups with or without addition of excess unlabeled AgRP at a dose usually effective in inhibiting saturable transport across the BBB (35). There was a significant effect of excess unlabeled AgRP [$F(1, 14) = 6.1$, $p < 0.05$]. Such an inhibitory effect suggests that the influx of AgRP from blood to liver was a saturable process.

The adrenal gland had the second highest influx rate (12.69 ± 1.48 μl/g-min), but this was seven-fold lower than that of the liver. The adrenal gland, however, had the highest initial volume of distribution (655.0 ± 35.50 μl/g). Excess unlabeled AgRP significantly decreased the influx rate [$F(1,11) = 28.0$, $p < 0.001$] (Fig.2). The differential uptake of AgRP in various organs is shown in Table 1.

By contrast, the total brain had the lowest influx of $^{125}$I-AgRP (Ki = 0.14 ± 0.02 μl/g-min), which is still significantly higher than that of $^{131}$I-albumin (Ki = 0.02 ± 0.03 μl/g-min, a non-significant entry). Excess unlabeled AgRP did not show acute modulation of the influx rate of $^{125}$I-AgRP to the whole brain, as seen in Figure 3. The experiment was repeated an additional three times with either the same or higher doses (2 and 5 μg/mouse) of unlabeled competitor. Addition of excess unlabeled AgRP did not affect the minimal influx of $^{131}$I-albumin, indicating that it did not change the vascular space or alter general vascular permeability. We also noted that specific brain regions

(hypothalamus and striatum) appeared to have saturable influx of $^{125}$I-AgRP and are further investigating this with multiple approaches.

**2. AgRP was relatively stable even in liver 10 min after intravenous delivery**

Figure 4 is a chromatograph of radioactivity in liver homogenate obtained 10 min after intravenous injection of $^{125}$I-AgRP. This correlates with that of the $^{125}$I-AgRP stock solution (inset). The major peak (fractions 18 – 24) correlated with intact $^{125}$I-AgRP from the stock solution and had an acid precipitability of 98%. This accounted for 83% of the radioactivity recovered in the liver. The minor peak (fraction 2) correlated with free $^{125}$I that was not acid precipitable and accounted for 3.6% of the total radioactivity recovered.

**3. Compartmental distribution showed that significantly more $^{125}$I-AgRP entered brain parenchyma than did $^{131}$I-albumin (Fig.5)**

Capillary depletion studies were performed on samples from mice 10 min after intravenous injection of $^{125}$I-AgRP. At this time, there was a moderate uptake of $^{125}$I-AgRP into the brain (12.60 ± 0.78 μl/g), higher than $^{125}$I-AgRP retained in the cerebral vasculature (3.91 ± 0.81 μl/g). Nonetheless, after cardiac perfusion over 50% of the total amount of AgRP in the perfused brain (5.67 ± 0.42 μl/g) was present in the parenchymal fraction (3.00 ± 0.18 μl/g). This is significantly ($p < 0.001$) higher than the minimal entry of $^{131}$I-albumin (0.41 ± 0.05 μl/g). Since brain is the organ with the least influx of AgRP in the presence of the BBB, it is conceivable that larger amounts of $^{125}$I-AgRP have entered the parenchyma of peripheral organs.

**4. Fasting selectively caused a significant increase of $^{125}$I-AgRP uptake by epididymal fat and liver and a decrease in the adrenal gland**

Similar to what was seen in the differential influx of $^{125}$I-AgRP in various organs over time, the uptake of $^{125}$I-AgRP at 10 min after intravenous delivery had great variation from organ to organ. This was seen in both fed and fasted mice. In mice fed a normal diet, the liver had the highest volume of distribution (1619.9 ± 59.9 μl/g). In the fasted group, the volume of distribution of $^{125}$I-AgRP in the liver was 2076.8 ± 76.7 μl/g. These values were not corrected for those of albumin. The difference between the two groups was significant [$F(1,7) = 22.8$, $p < 0.005$]. Similarly, epididymal fat had a volume of distribution of 37.0 ± 1.7 μl/g in the fed mice and 57.8 ± 7.2 μl/g in the fasted mice. The difference between the two groups was also significant [$F(1,7) = 9.9$, $p < 0.05$].

By contrast to the increased uptake of $^{125}$I-AgRP in liver and epididymal fat after overnight fasting, the adrenal gland had a significant reduction ($p < 0.05$) of the volume of distribution of $^{125}$I-AgRP, from 1068.8 ± 95.4 μl/g to 797.7 ± 59.1 μl/g. The rest of the organs tested (brain, muscle, testis, pancreas, lungs, and heart) showed no significant changes in the volume of distribution of $^{125}$I-AgRP after fasting (Fig.6).

To confirm the findings obtained from the C57 mice, a further experiment in CD1 mice was performed with a multiple-time regression analysis design. Figure 7A shows that the Ki in the liver was 53.77 ± 8.87 μl/g-min and 80.52 ± 7.82 μl/g-min in the fed and fasted groups, respectively, and their corresponding initial volume of distribution was 356.9 ± 112.5 μl/g and 451.6 ± 122.4 μl/g. The difference between the Ki values was significant

[F(1,14) = 5.1, $p < 0.05$]. The epididymal fat had a significant increase in the Vi [F(1,15) = 7.3, $p < 0.05$] as shown in Fig.7B. By contrast, the adrenal gland had a significant decrease in the Vi [F(1,15) = 7.3, $p < 0.05$] (Fig.7C). The results are consistent with those seen in the single-time uptake studies above.

## DISCUSSION

Our previous study showed that human $^{125}$I-AgRP aggregates in blood and permeates the BBB slowly (21). There was no saturable influx or efflux transport system for the brain. Supported by accumulating evidence that peripheral AgRP could be involved in important physiological functions, and that endogenous AgRP protein is detectable in the blood circulation, we further determined the kinetics of mouse AgRP influx from blood to tissue. In addition, we showed that AgRP was selectively taken up by various organs in the mouse and this uptake was further modulated by fasting.

Since the full-length AgRP is not currently available commercially, we used a bioactive C-terminal fragment. Although its pharmacokinetic profile might differ slightly from that of full-length AgRP, it binds to the same receptors and its Ki and Vi should reflect the specific uptake of AgRP which is present in the blood circulation physiologically. We first determined the pattern of serum disappearance after an intravenous bolus injection of $^{125}$I-AgRP. The kinetics fit a one-phase exponential decay model, indicating that there was no significant redistribution of $^{125}$I-AgRP in peripheral organs during the study period. The serum half-life was comparable to that of some large proteins we have studied (36). This is consistent with reports that $^{125}$I-AgRP can polymerize in blood (21),

and that endogenous AgRP in the rat can be detected by HPLC and ion-exchange chromatography (37). Since $^{125}$I-AgRP (82-131) was relatively stable in blood and tissue and the influx was linear within the first 30 min, we were able to calculate the Ki and Vi by standard methods established by us and others over the past two decades (31;32;38).

Of all the tissues tested, liver had the fastest influx rate of AgRP(82-131) and the adrenal gland had the highest initial volume of distribution. The capillaries in the liver are fenestrated and this can explain the high permeability to both $^{125}$I-AgRP and the vascular space marker $^{131}$I-albumin. Even though the liver is the main organ of degradation because of its large supply of enzymes, HPLC showed that the radioactivity in liver homogenate mainly represented intact $^{125}$I-AgRP, even 10 min after intravenous injection. Therefore, the high uptake of AgRP by the liver was explained by its permeation rather than by accumulation of degraded peptide. The distribution of mRNA for AgRP (25) and melanocortin receptors (24;39) have been mapped in chicken. Both AgRP and MC4R are highly expressed in the liver. These results suggest that the selective uptake of AgRP(82-131) by the liver is probably mediated by the melanocortin receptors.

The adrenal gland and fat tissue also express high levels of melanocortin receptors (39). The adrenal gland had the highest volume of distribution despite a moderately high influx rate; this is probably related to the abundant binding sites of $^{125}$I-AgRP in this organ. The adrenal gland is a major site of AgRP production and action (30). MC3R and MC4R expression has been shown in the rat adrenal gland (28) and MC4R expression in rat

heart, lungs, kidney, and testis (29). Further evidence that the specific uptake is independent of vascular permeability and vascular space was shown by the lack of correlation between the Ki and regional blood flow (40;41).

Consistent with our previous study with the human AgRP fragment in mice (21), murine AgRP (82-131)-$NH_2$ had very limited entry into brain parenchyma. Capillary depletion studies in the cerebral cortex after removal of residual radioactivity in the vascular bed showed that about 50% of $^{125}$I-AgRP in the brain actually entered parenchyma at 10 min. This limited uptake was not mediated by a specific transport system to the whole brain as shown by the lack of effect of excess unlabeled AgRP. This indicates that high concentrations of circulating AgRP may have a better chance of permeating the BBB than if a saturable system limited access to the CNS by the constraints of a ceiling effect.

Having observed the differential uptake of $^{125}$I-AgRP in various organs, we further examined the changes after overnight fasting. The minimal uptake in the whole brain was not affected by food withdrawal; however both epididymal fat and liver had a significantly higher uptake when compared with these organs in the fed mice. By contrast, the adrenal gland had a significant decrease in the uptake of $^{125}$I-AgRP 10 min after intravenous injection. We propose that the changes in the saturable entry of $^{125}$I-AgRP, seen in the liver and adrenal gland, were related to fasting-induced metabolic changes in these organs. In support of this possibility, we have shown that fasting increases mRNA expression of AgRP in hypothalamus and adrenal gland, but decreases AgRP mRNA in epididymal fat (30). Therefore, fasting-modulated endogenous AgRP expression in the organs could directly affect the pharmacokinetics of blood-borne AgRP.

To summarize, we used AgRP(82-131), a bioactive fragment commonly used in pharmacological studies, to determine the tissue-specific influx from blood where AgRP can be detected in physiological conditions. We found that peripheral organs had selective uptake of AgRP(82-131) at different rates, and that the influx was fastest in the liver, followed by adrenal gland, then heart, lungs, and skeletal muscle. There was saturation of the influx in the liver and adrenal gland at the dose tested. Such specificity coincided with organ-selective changes of AgRP uptake after overnight fasting. Tissue specificity was further reflected by the significant increase of AgRP uptake by liver and epididymal fat and significant decrease by the adrenal gland. Therefore, although single bolus peripheral AgRP may not exert a potent acute effect on food intake and energy expenditure as centrally administered AgRP does (18;22;42), it could still play important regulatory roles in situations such as food deprivation.

**ACKNOWLEDGEMENTS**

Supported by NIH (NS45751 and NS46528 to WP, DK54880 and AA12865 to AJK, and DK62156 to GA).

**REFERENCES**

1. Katsuki A, Sumida Y, Gabazza EC, Murashima S, Tanaka T, Furuta M, Araki-Sasaki R, Hori Y, Nakatani K, Yano Y, Adachi Y 2001 Plasma levels of agouti-related protein are increased in obese men. J Clin Endocrinol Metab 86:1921-1924
2. Shen CP, Wu KK, Shearman LP, Camacho R, Tota MR, Fong TM, Van der Ploeg LH 2002 Plasma agouti-related protein level: a possible correlation with fasted and fed States in humans and rats. J Neuroendocrinol 14:607-610

3. Hoggard N, Johnston AM, Faber P, Gibney ER, Elia M, Lobley G, Rayner V, Horgan G, Hunter L, Bashir S, Stubbs RJ 2004 Plasma concentrations of alpha-MSH, AgRP and leptin in lean and obese men and their relationship to differing states of energy balance perturbation. Clin Endocrinol 61:31-39

4. Friedman JM 2000 Obesity in the new millennium. Nature 404:632-634

5. Schwartz MW, Woods SC, Porte D Jr, Seeley RJ, Baskin DG 2000 Central nervous system control of food intake. Nature 404:661-671

6. Schwartz MW 2001 Brain pathways controlling food intake and body weight. Exp Biol Med 226:978-981

7. Mayfield DK, Brown AM, Page GP, Garvey WT, Shriver MD, Argyropoulos G 2001 A role for the agouti related protein promoter in obesity and type 2 diabetes. Biochem Biophys Res Commun 287:568-573

8. Argyropoulos G, Rankinen T, Neufeld DR, Rice T, Province MA, Leon AS, Skinner JS, Wilmore JH, Rao DC, Bouchard C 2002 A polymorphism in the human agouti-related protein is associated with late-onset obesity. J Clin Endocrinol Metab 87:4198-4202

9. Argyropoulos Geal, Rankinen T, Bai F, Rice T, Province MA, Leon AS, Skinner JS, Wilmore JH, Rao DC, Bouchard C 2003 The agouti related protein and body fatness in humans. Int J Obes 27:276-280

10. Broberger C, Johansen J, Johansson C, Schalling M, Hokfelt T 1998 The neuropeptide Y/agouti gene-related protein (AGRP) brain circuitry in normal, anorectic, and monosodium glutamate-treated mice. Proc Natl Acad Sci 95:15043-15048

11. Hanada R, Nakazato M, Matsukura S, Murakami N, Yoshimatsu H, Sakata T 2005 Differential regulation of melanin-concentrating hormone and orexin genes in the agouti-related protein/melanocortin-4 receptor system. Biochem Biophys Res Commun 268:88-91

12. Baskin DG, Hahn TM, Schwartz MW 1999 Leptin sensitive neurons in the hypothalamus. Hormone Metab Res 31:345-350

13. Wilson BD, Ollmann MM, Barsh GS 1999 The role of agouti-related protein in regulating body weight. Mol Med Today 5:250-256

14. Graham M, Shutter JR, Sarmiento U, Sarosi I, Stark KL 1997 Overexpression of AGRP leads to obesity in transgenic mice. Nature Genetics 17:273-274

15. Rossi M, Kim MS, Morgan DGA, Small CJ, Edwards CMB, Sunter D, Abusnana S, Goldstone AP, Russell SH, Stanley SA, Smith DM, Yagaloff K, Ghatei MA, Bloom SR 1998 A C-terminal fragment of Agouti-related protein increases feeding and

antagonizes the effect of alpha-melanocyte stimulating hormone in vivo. Endocrinol 139:4428-4431

16. Hagan MM, Rushing PA, Pritchard LM, Schwartz MW, Strack AM, Van der Ploeg LHT, Woods SC, Seeley RJ 2000 Long-term orexigenic effects of AgRP-(83-132) involve mechanisms other than melanocortin receptor blockade. Am J Physiol 279:R47-R52

17. Small CJ, Liu YL, Stanley SA, Connoley IP, Kennedy A, Stock MJ, Bloom SR 2003 Chronic CNS administration of agouti-related protein (Agrp) reduces energy expenditure. Int J Obes 27:530-533

18. Tang-Christensen M, Vrang N, Ortmann S, Bidlingmaier M, Horvath TL, Tschop M 2004 Central administration of ghrelin and agouti-related protein (83-132) increases food intake and decreases spontaneous locomotor activity in rats. Endocrinol 145:4645-4652

19. Goto K, Inui A, Takimoto Y, Yuzuriha H, Asakawa A, Kawamura Y, Tsuji H, Takahara Y, Takeyama C, Katsuura G, Kasuga M 2003 Acute intracerebroventricular administration of either carboxyl-terminal or amino-terminal fragments of agouti-related peptide produces a long-term decrease in energy expenditure in rats. Intl J Mol Med 12:379-383

20. Yang YK, Thompson DA, Dickinson CJ, Wilken J, Barsh GS, Kent SBH, Gantz I 1999 Characterization of Agouti-related protein binding to melanocortin receptors. Mol Endocrinol 13:148-155

21. Kastin AJ, Akerstrom V, Hackler L 2000 Agouti-related protein(83-132) aggregates and crosses the blood-brain barrier slowly. Metab 49:1444-1448

22. Hoggard N, Rayner DV, Johnston SL, Speakman JR 2004 Peripherally administered [$Nle^4$, D-$Phe^7$]-α-melanocyte stimulating hormone increases resting metabolic rate, while peripheral agouti-related protein has no effect, in wild type C57BL/6 and *ob/ob* mice. J Mol Endocrinol 33:693-703

23. Shutter JR, Graham M, Kinsey AC, Scully S, Luthy R, Stark KL 1997 Hypothalamic expression of ART, a novel gene related to agouti, is up- regulated in obese and diabetic mutant mice. Genes Dev 11:593-602

24. Takeuchi S, Takahashi S 1999 A possible involvement of melanocortin 3 receptor in the regulation of adrenal gland function in the chicken. Biochim Biophys Acta 1448:512-518

25. Takeuchi S, Teshigawara K, Takahashi S 2000 Widespread expression of Agouti-related protein (AGRP) in the chicken: a possible involvement of AGRP in regulating peripheral melanocortin systems in the chicken. Biochim Biophys Acta 1496:261-269

26. Doghman Mea, Delagrange P, Berthelon MC, Durand P, Naville D, Begeot M 2005 Sustained inhibitory effect of Agouti Related Protein on the ACTH-induced cortisol production by bovine cultured adrenal cells. Regul Peptides 124:215-219

27. Xiang L, Murai A, Muramatsu T 2004 The effects of agouti-related protein gene transfer in vivo by electroporation in mice. Neurosci Lett 370:108-113

28. Dhillo WS, Small CJ, Gardiner.J.V., Bewick GA, Whitworth EJ, Jethwa PH, Seal LJ, Ghatei MA, Hinson JP, Bloom SR 2003 Agouti-related protein has an inhibitory paracrine role in the rat adrenal gland. Biochem Biophys Res Commun 301:102-107

29. Mountjoy KG, Wu CSJ, Dumont LM, Wild JM 2003 Melanocortin-4 receptor messenger ribonucleic acid expression in rat cardiorespiratory, musculoskeletal, and integumentary systems. Endocrinol 144:5488-5496

30. Charbonneau C, Bai F, Richards BS, Argyropoulos G 2004 Central and Peripheral Interactions Between the Agouti Related Protein and Leptin. Biochem Biophys Res Commun 319:518-524

31. Blasberg RG, Fenstermacher JD, Patlak CS 1983 Transport of α-aminoisobutyric acid across brain capillary and cellular membranes. J Cereb Blood Flow Metab 3:8-32

32. Kastin AJ, Akerstrom V, Pan W 2001 Validity of multiple-time regression analysis in measurement of tritiated and iodinated leptin crossing the blood-brain barrier: meaningful controls. Peptides 22:2127-2136

33. Banks WA, Robinson SM, Verma S, Morley JE 2003 Efflux of human and mouse amyloid β proteins 1-40 and 1-42 from brain: impairment in a mouse model of Alzheimer's disease. Neurosci 121:487-492

34. Pan W, Banks WA, Kastin AJ 1998 Permeability of the blood-brain barrier to neurotrophins. Brain Res 788:87-94

35. Pan W, Kastin AJ, Brennan JM 2000 Saturable entry of leukemia inhibitory factor from blood to the central nervous system. J Neuroimmunol 106:172-180

36. Pan W, Kastin AJ, Zankel T, van Kerkhof P, Terasaki T, Bu G 2004 Efficient transfer of receptor-associated protein (RAP) across the blood-brain barrier. J Cell Sci 117:5071-5078

37. Li JY, Finniss S, Yang YK, Zeng Q, Qu SY, Barsh G, Dickinson C, Gantz I 2000 Agouti-related protein-like immunoreactivity: characterization of release from hypothalamic tissue and presence in serum. Endocrinol 141:1942-1950

38. Banks WA, Kastin AJ 1993 Measurement of transport of cytokines across the blood-brain barrier. Methods Neurosci 16:67-77

39. Takeuchi S, Takahashi S 1998 Melanocortin receptor genes in the chiken - tissue distributions. General Comp Endocrinol 112:220-231

40. Crandall DL, Goldstein BM, Gabel RA, Cervoni P 1984 Hemodynamic effects of weight reduction in the obese rat. Am J Physiol 247:R266-R271

41. Ma SWY, Foster DO 1986 Starvation-induced changes in metabolic rate, blood flow, and regional energy expenditure in rats. Can J Phyiol Pharmacol 64:1252-1258

42. Ebihara K, Ogawa Y, Katsuura G, Numata Y, Masuzaki H, Satoh N, Tamaki M, Yoshioka T, Hayase M, Matsuoka N, Aizawa-Abe M, Yoshimasa Y, Nakao K 1999 Involvement of agouti-related protein, an endogenous antagonist of hypothalamic melanocortin receptor, in leptin action. Diabetes 48:2028-2033

**FIGURE LEGENDS**

Fig.1 The liver had the most rapid influx rate of $^{125}$I-AgRP. Inclusion of 1 μg/mouse of excess AgRP caused a significant decrease in the Ki ($p < 0.05$).

Fig.2 $^{125}$I-AgRP was taken up rapidly by the adrenal gland. Excess unlabeled AgRP caused a significant inhibition of the influx [$F(1,11) = 28.0$, $p < 0.001$].

Fig.3 The influx of $^{125}$I-AgRP into the brain was significantly higher than that of albumin but it was not inhibitable by excess unlabeled AgRP.

Fig.4. HPLC profile of the supernatant from liver homogenate 10 min after iv injection of $^{125}$I-AgRP. The major peak correlated with that of the intact $^{125}$I-AgRP in the stock solution (shown in inset).

Fig.5 At 10 min after iv injection, substantial amount of $^{125}$I-AgRP entered brain parenchyma and accounted for over 50% of radiotracer in the perfused brain.

Fig.6 After overnight fasting, the uptake of $^{125}$I-AgRP (10 min after iv injection) was significantly higher in the liver and epididymal fat, and lower in the adrenal gland, when the fasted mice ($n = 4$) were compared with the fed mice ($n = 5$).

Fig.7A Overnight fasting significantly increased the Ki of $^{125}$I-AgRP into the liver [$F(1,14) = 5.1$, $p < 0.05$].

Fig.7B The Vi of $^{125}$I-AgRP in epididymal fat was significantly increased by overnight fasting [$F(1,15) = 7.3$, $p < 0.05$] although the Ki was not changed.

Fig.7C The Vi of $^{125}$I-AgRP in the adrenal gland was significantly decreased by fasting [$F(1,15) = 7.3$, $p < 0.05$] although there was no change in Ki.

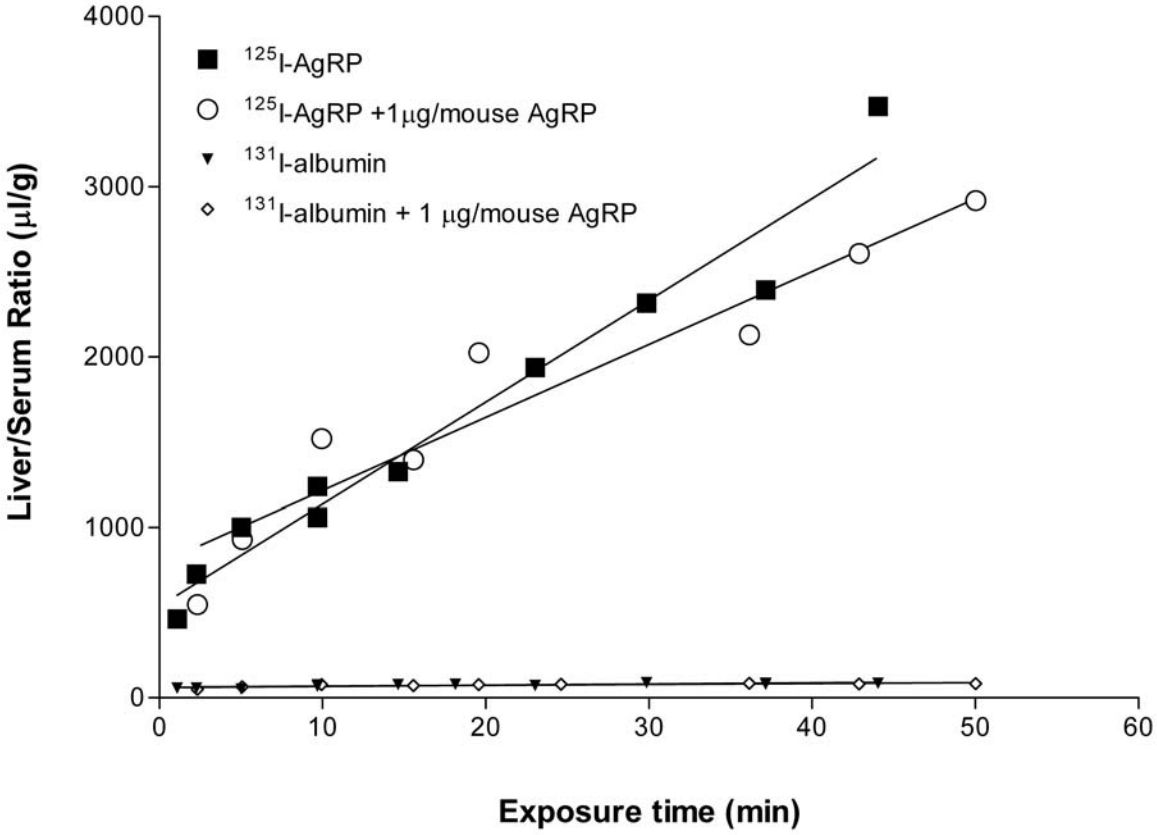


Fig.1 The liver had the most rapid influx rate of $^{125}$I-AgRP. Inclusion of 1 μg/mouse of excess AgRP caused a significant decrease in the Ki ($p < 0.05$).

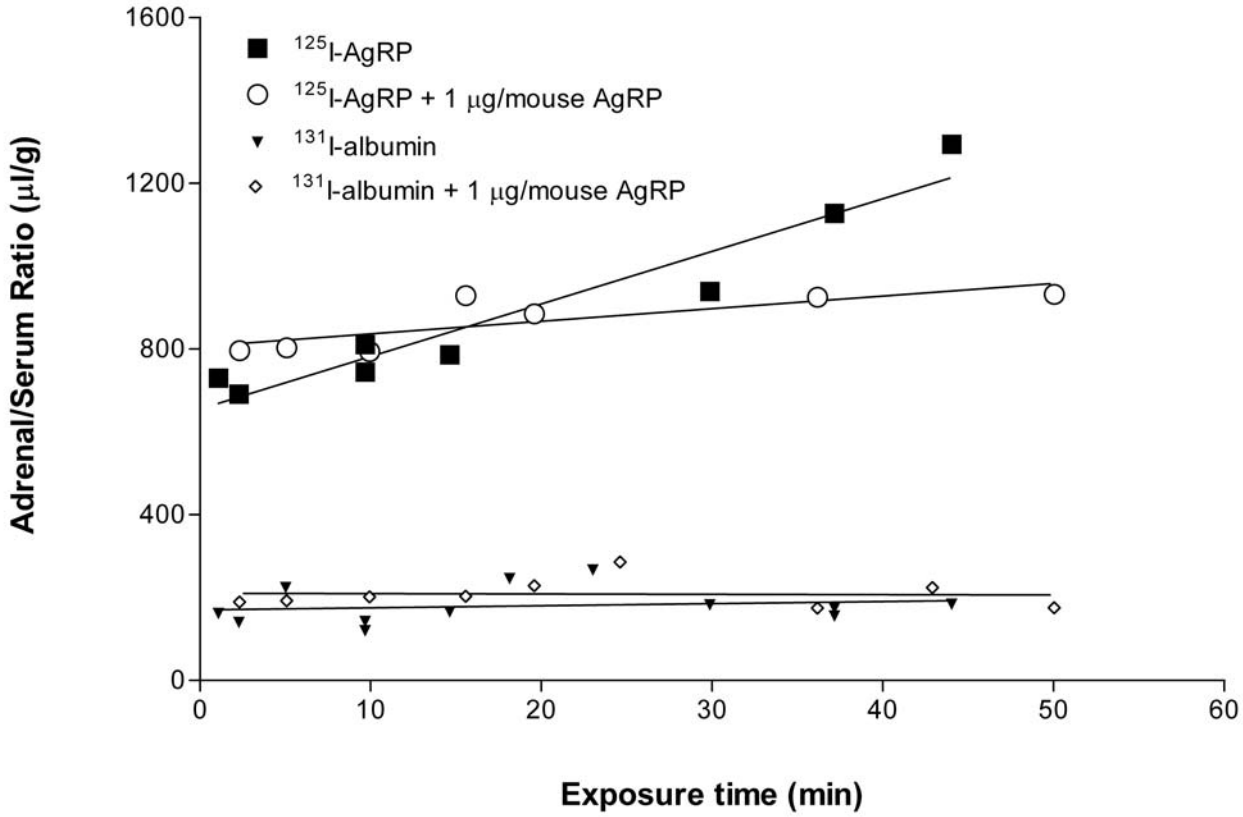


Fig.2. $^{125}$I-AgRP was taken up rapidly by the adrenal gland. Excess unlabeled AgRP caused a significant inhibition of the influx [$F(1,11) = 28.0$, $p < 0.001$].

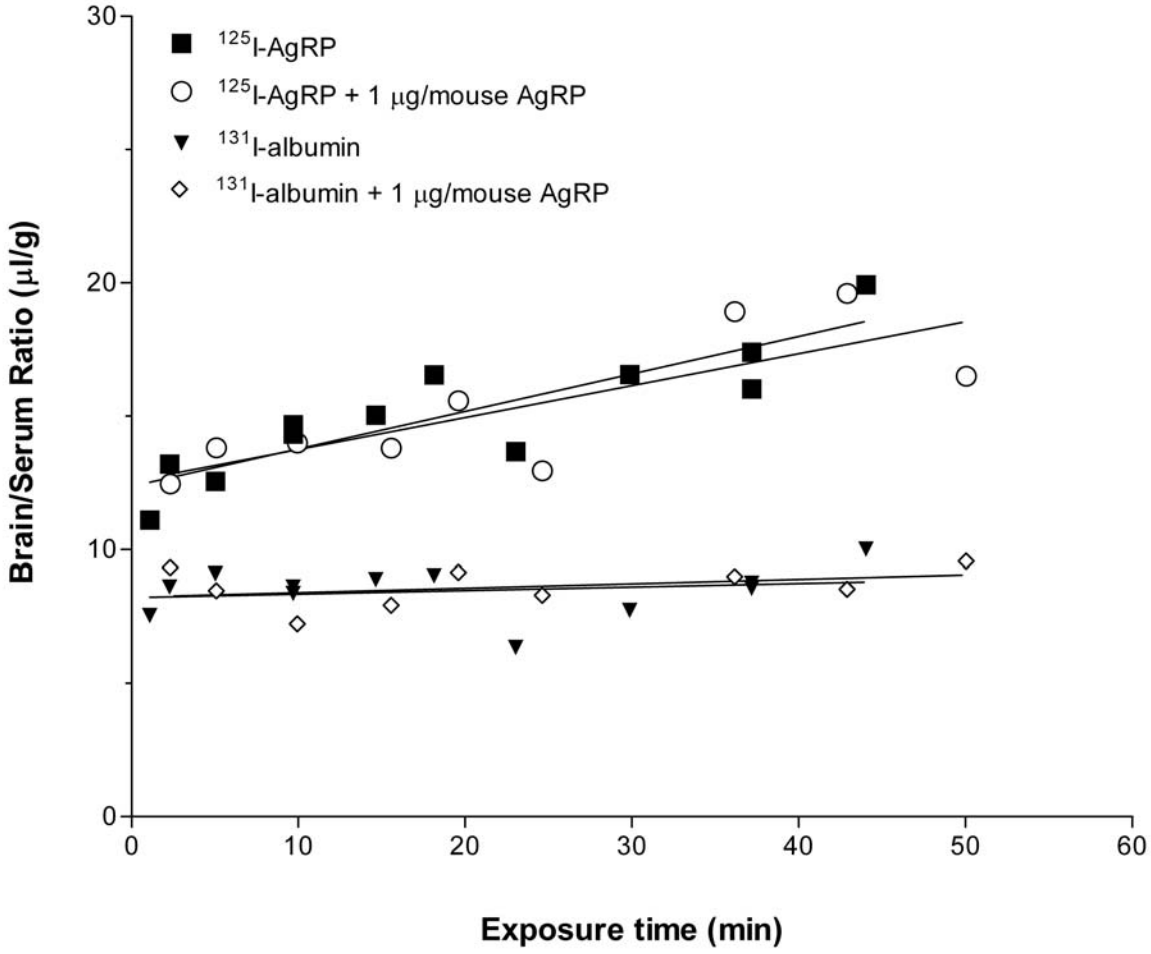


Fig.3 The influx of $^{125}$I-AgRP into the brain was significantly higher than that of albumin but it was not inhibitable by excess unlabeled AgRP.

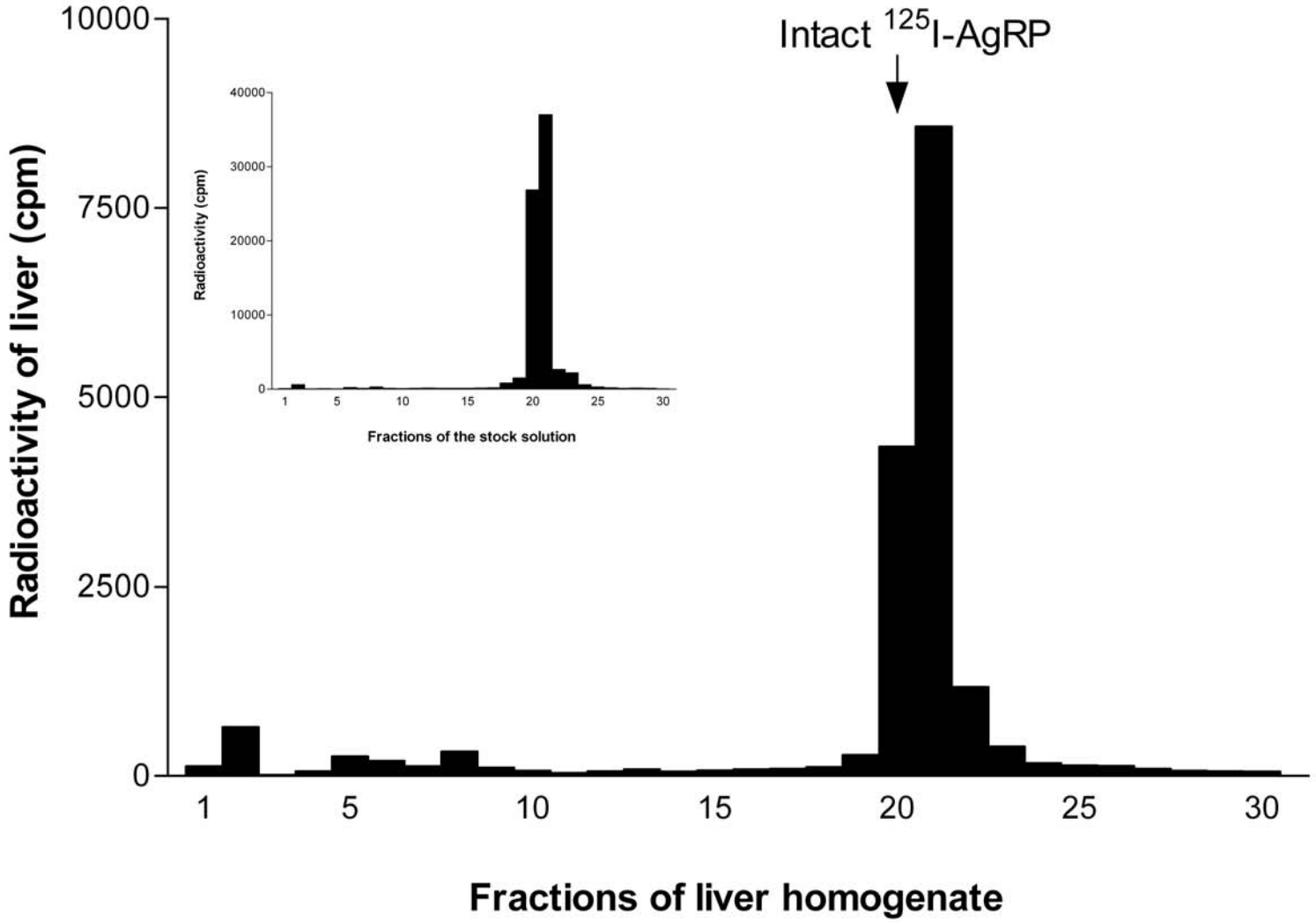


Fig.4. HPLC profile of the supernatant from liver homogenate 10 min after iv injection of $^{125}$I-AgRP. The major peak correlated with that of the intact $^{125}$I-AgRP in the stock solution (shown in inset).

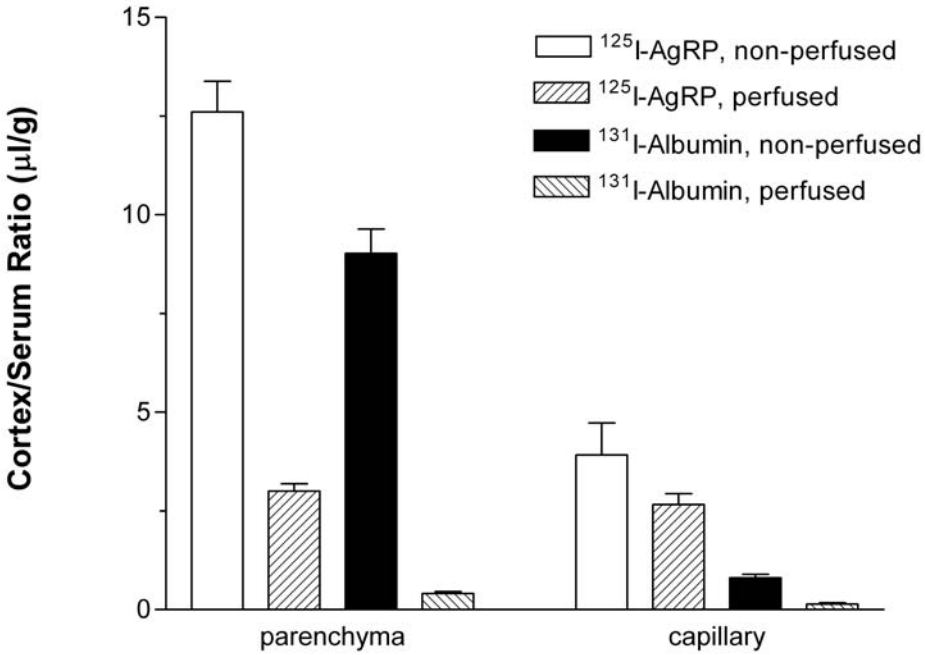


Fig.5. At 10 min after iv injection, substantial amount of $^{125}$I-AgRP entered brain parenchyma and accounted for over 50% of radiotracer in the perfused brain.

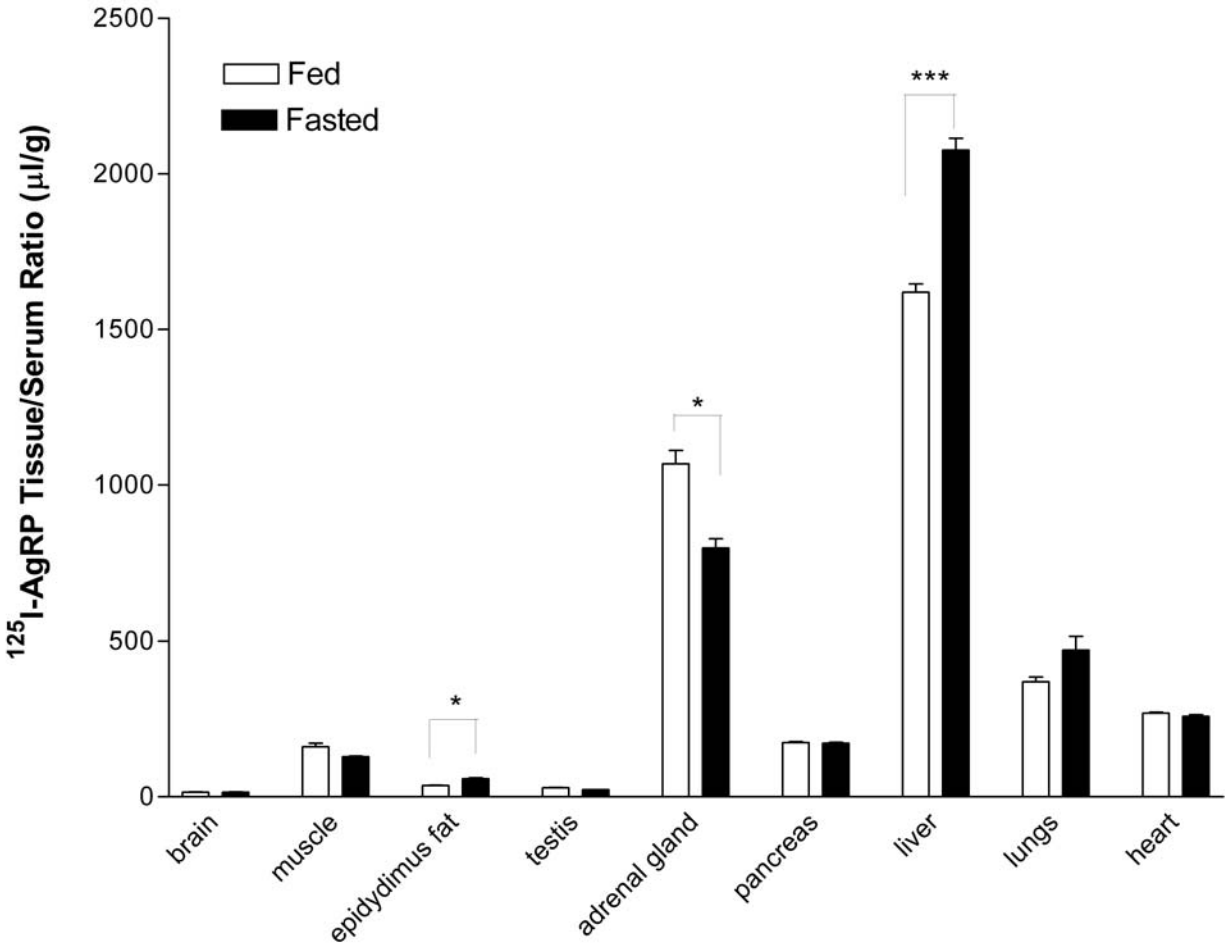


Fig.6. After overnight fasting, the uptake of $^{125}$I-AgRP (10 min after iv injection) was significantly higher in the liver and epididymus fat, and lower in the adrenal gland, when the fasted mice (n = 4) were compared with the fed mice (n = 5).

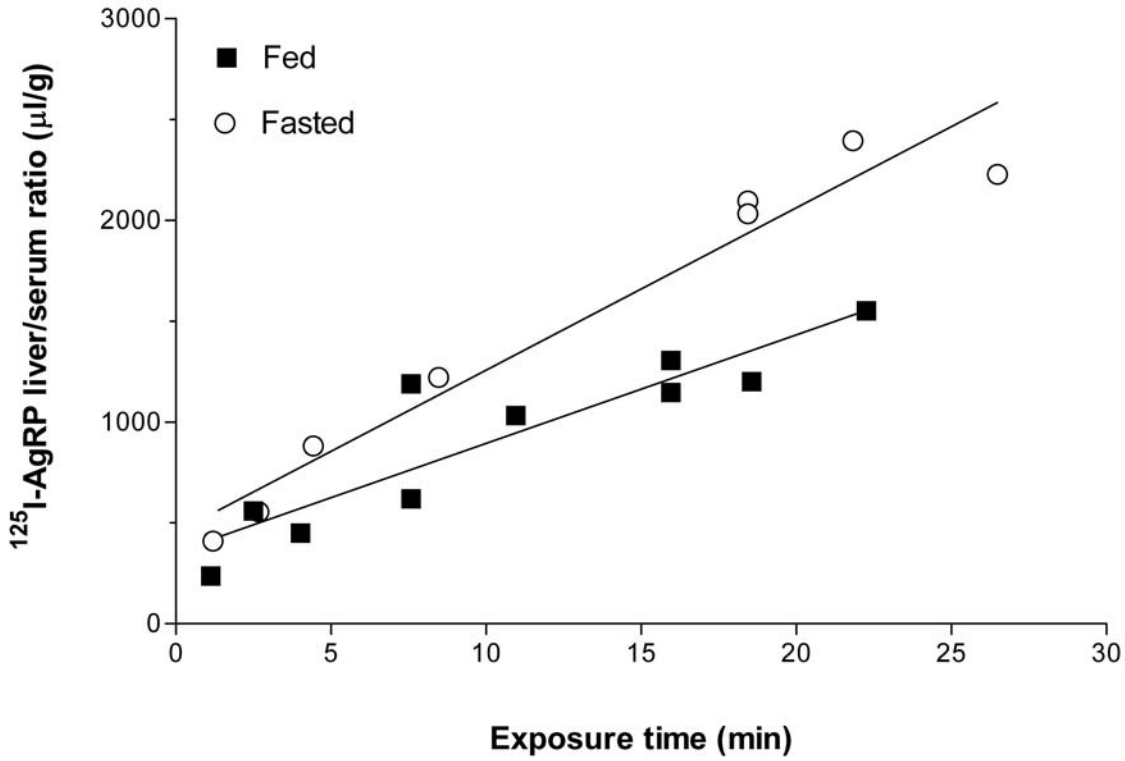


Fig.7A. Overnight fasting significantly increased the Ki of $^{125}$I-AgRP into the liver [$F(1,14) = 5.1$, $p < 0.05$].

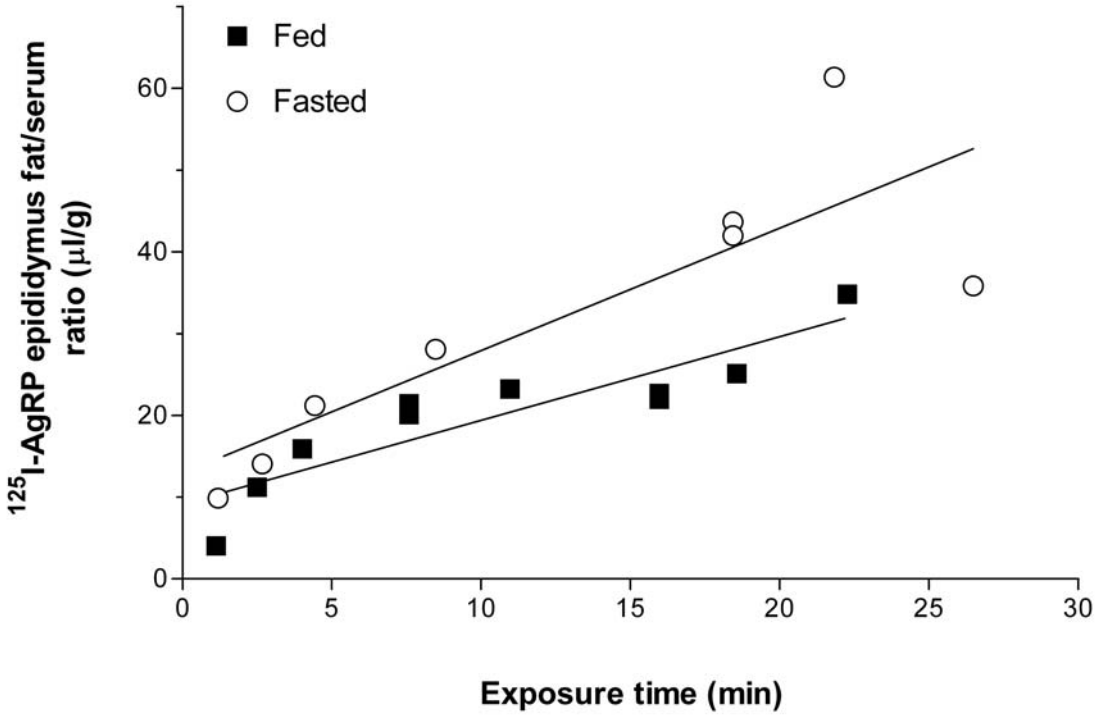


Fig.7B. The Vi of $^{125}$I-AgRP in epididymal fat was significantly increased by overnight fasting [$F(1,15) = 7.3$, $p < 0.05$] although the Ki was not changed.

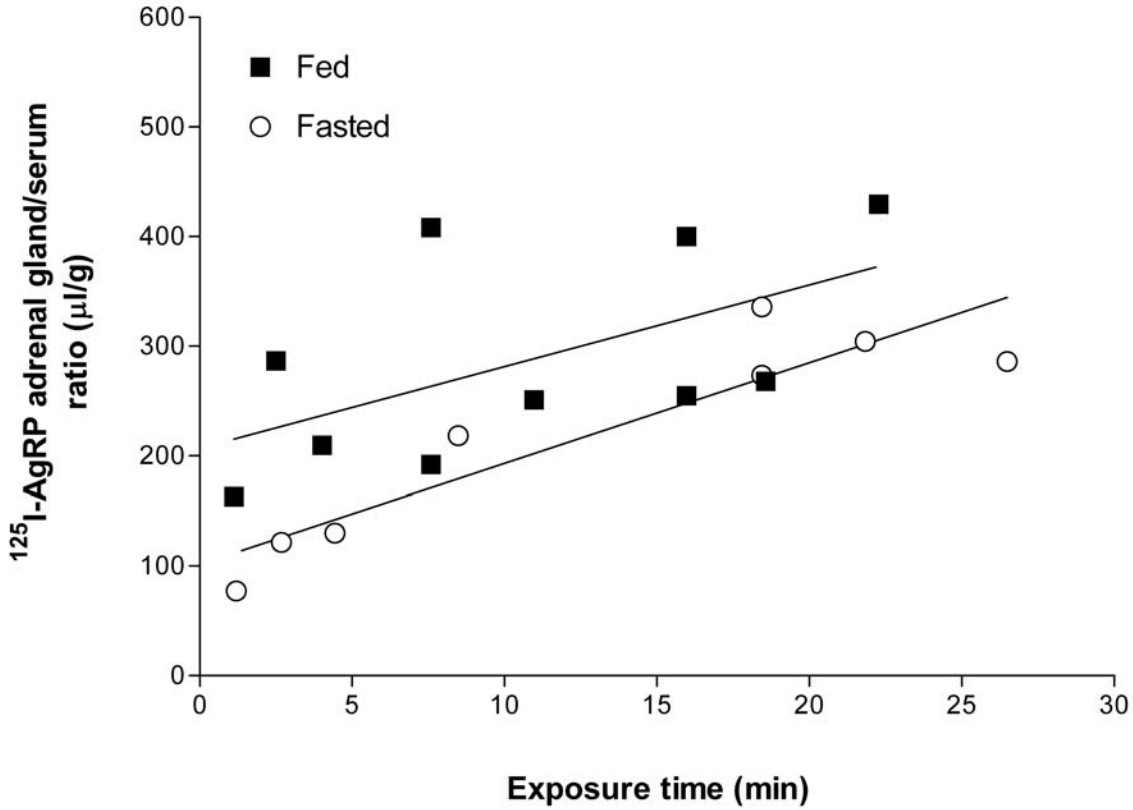


Fig.7C. The Vi of $^{125}$I-AgRP in the adrenal gland was significantly decreased by fasting [$F(1,15) = 7.3$, $p < 0.05$] although there was no change in Ki.